

## ON A NEW NEAR-INFRARED METHOD TO ESTIMATE THE ABSOLUTE AGES OF STAR CLUSTERS: NGC 3201 AS A FIRST TEST CASE<sup>1</sup>

G. BONO<sup>2,3</sup>, P. B. STETSON<sup>4</sup>, D. A. VANDENBERG<sup>5</sup>, A. CALAMIDA<sup>6</sup>, M. DALL'ORA<sup>7</sup>, G. IANNICOLA<sup>3</sup>, P. AMICO<sup>6</sup>, A. DI CECCO<sup>2</sup>, E. MARCHETTI<sup>6</sup>, M. MONELLI<sup>8</sup>, N. SANNA<sup>2</sup>, A. R. WALKER<sup>9</sup>, M. ZOCCALI<sup>10</sup>, R. BUONANNO<sup>2</sup>, F. CAPUTO<sup>3</sup>, C. E. CORSI<sup>3</sup>, S. DEGL'INNOCENTI<sup>11,12</sup>, S. D'ODORICO<sup>6</sup>, I. FERRARO<sup>3</sup>, R. GILMOZZI<sup>6</sup>, J. MELNICK<sup>6</sup>, M. NONINO<sup>13</sup>, S. ORTOLANI<sup>14</sup>, A. M. PIERSIMONI<sup>15</sup>, P. G. PRADA MORONI<sup>11,12</sup>, L. PULONE<sup>3</sup>, M. ROMANIELLO<sup>6</sup>, AND J. STORM<sup>16</sup>

(Dated: drafted November 4, 2018 / Received / Accepted)  
*Draft version November 4, 2018*

### ABSTRACT

We present a new method to estimate the absolute ages of stellar systems. This method is based on the difference in magnitude between the main sequence turn-off (MSTO) and a well defined knee located along the lower main sequence (MSK). This feature is caused by the collisionally induced absorption of molecular hydrogen and it can be easily identified in near-infrared (NIR) and in optical-NIR color-magnitude diagrams of stellar systems. We took advantage of deep and accurate NIR images collected with the Multi-Conjugate Adaptive Optics Demonstrator temporarily available on the Very Large Telescope and of optical images collected with the Advanced Camera for Surveys Wide Field Camera on the Hubble Space Telescope and with ground-based telescopes to estimate the absolute age of the globular NGC 3201 using both the MSTO and the  $\Delta$ (MSTO-MSK). We have adopted a new set of cluster isochrones and we found that the absolute ages based on the two methods agree to within one sigma. However, the errors of the ages based on the  $\Delta$ (MSTO-MSK) method are potentially more than a factor of two smaller, since they are not affected by uncertainties in cluster distance or reddening. Current isochrones appear to predict slightly bluer ( $\approx 0.05$  mag) NIR and optical-NIR colors than observed for magnitudes fainter than the MSK.

*Subject headings:* globular clusters: individual (NGC3201) — stars: evolution — stars: fundamental parameters

### 1. INTRODUCTION

The absolute ages of Galactic Globular Clusters (GGCs) is a crossroad of several astrophysical problems (VandenBerg et al. 1996; Chaboyer 1998; Castellani 1999). This parameter provides: *i*) a lower limit to the age of the universe (Buonanno et al. 1998; Stetson et al. 1999; Gratton et al. 2003); *ii*) robust constraints on the

physics adopted in stellar evolutionary models (Salaris & Weiss 1998; Cassisi et al. 1999; VandenBerg et al. 2008; Dotter et al. 2008), and *iii*) the chronology for the assembly of the halo, bulge and disk of the Milky Way (Carraro et al. 1999; Rosenberg et al. 1999; Zoccali et al. 2003; de Angeli et al. 2005). However, estimates of absolute GC ages are still hampered by uncertainties in the distance, extinction and the reddening law (Renzini 1991; Bono et al. 2008), the overall metallicity scale (Rutledge et al. 1997; Kraft & Ivans 2003), as well as the detailed distribution of heavy-element abundances (Asplund et al. 2005), and photometric zero-points (Stetson 2000).

Proposed ways of overcoming some of these thorny problems include the use either of a different clock (white dwarf cooling sequence, Richer et al. 2006), or different photometric systems (Strömgren bands, Grundahl et al. 1998) or different diagnostics (luminosity function, Zoccali et al. 2000; Richer et al. 2008). However, these alternative approaches to estimate the absolute ages of GCs can be impeded by limiting magnitude, by photometric accuracy, or by sample completeness. Simultaneous and self-consistent interpretation of optical and NIR photometry is another way to refine current distance and reddening estimates. In fact, as shown in this study (see also Calamida et al. 2009) deep  $J, K$  photometry reveals the existence of a well-defined “knee” in the lower main sequence. The position of this feature is, at fixed chemical composition, essentially independent of the cluster age. Therefore, the difference either in magnitude or in color with the turn-off can provide robust estimates of the absolute age.

Consider the GC NGC 3201, which has several inter-

<sup>1</sup> Based on near infrared observations made with ESO telescopes SOFI@NTT, La Silla; MAD@VLT Paranal, projects: 66.D-0557, 074.D-0655, ID96406 and with the CTIO telescope ISPI@4m Blanco, La Serena. Based on optical data collected with ESO telescopes and retrieved from the ESO Science Archive Facility. This research used the facilities of the Canadian Astronomy Data Centre operated by the National Research Council of Canada with the support of the Canadian Space Agency.

<sup>2</sup> Dept. of Physics, UniToV, via della Ricerca Scientifica 1, 00133 Rome, Italy; bono@roma2.infn.it

<sup>3</sup> INAF-OAR, via Frascati 33, Monte Porzio Catone, Rome, Italy

<sup>4</sup> DAO-HIA, NRC, 5071 West Saanich Road, Victoria, BC V9E 2E7, Canada

<sup>5</sup> Dept. of Physics and Astronomy, UVIC, Victoria, BC V8W 3P6, Canada

<sup>6</sup> ESO, Karl-Schwarzschild-Str. 2, 85748 Garching bei Munchen, Germany

<sup>7</sup> INAF-OACN, via Moiarriello 16, 80131 Napoli, Italy

<sup>8</sup> IAC, Calle Via Lactea, E38200 La Laguna, Tenerife, Spain

<sup>9</sup> CTIO-NOAO, Casilla 603, La Serena, Chile

<sup>10</sup> PUC, Dept. Astronomia y Astrofisica, Casilla 306, Santiago 22, Chile

<sup>11</sup> Dept. of Physics, Univ. Pisa, Largo B. Pontecorvo 2, 56127 Pisa, Italy

<sup>12</sup> INFN, Sez. Pisa, via E. Fermi 2, 56127 Pisa, Italy

<sup>13</sup> INAF-OAT, via G.B. Tiepolo 11, 40131 Trieste, Italy

<sup>14</sup> Dept. of Astronomy, Univ. of Padova, Vicolo dell' Osservatorio 5, 35122 Padova, Italy

<sup>15</sup> INAF-OACTe, via M. Maggini, 64100 Teramo, Italy

<sup>16</sup> AIP, An der Sternwarte 16, D-14482 Potsdam, Germany

esting properties. It is relatively nearby and it suffers from appreciable foreground reddening ( $\mu = 13.32 \pm 0.06$ ,  $E(B - V) = 0.30 \pm 0.03$ , Piersimoni et al. 2002;  $\mu = 13.36 \pm 0.06$ ,  $E(B - V) = 0.25 \pm 0.02$ , Layden & Sarajedini 2003; Mazur et al. 2003). Accurate abundances estimates exist for both iron ( $[\text{Fe}/\text{H}] = -1.54 \pm 0.10$ , Kraft & Ivans 2003; Covey et al. 2003) and  $\alpha$ -elements ( $[\alpha/\text{Fe}] \sim 0.2\text{--}0.4$ , Pritzl et al. 2005). However, NGC 3201 is affected by field contamination and by differential reddening (Piersimoni et al. 2002; Kravtov et al. 2009). Owing to these problems, we still lack an accurate estimate of its absolute age (Layden & Sarajedini 2003).

## 2. OBSERVATIONS AND DATA REDUCTION

Near-Infrared (NIR) data ( $J, K_s$ ) were collected in two observing runs with different pointings of the NIR camera SOFI (Field of View [FoV]  $\sim 5' \times 5'$ ; scale  $0''.29$  /px) on the New Technology Telescope (NTT; ESO, La Silla). We obtained 132  $J$ -band images with individual exposure times from 3 to 6 s and median seeing  $0''.8$ . We also collected 161  $K_s$ -band images with exposure times from 10 to 12 s and median seeing  $0''.6$ . The total exposures per band are  $\approx 10$  ( $J$ ) and  $\approx 40$  minutes ( $K_s$ ). These images unevenly cover an area of  $\approx 20' \times 18'$  across the cluster center (see Fig. 1). NIR data ( $J, K_s$ ) were also collected with the NIR camera ISPI (FoV  $\sim 10'.5 \times 10'.5$ ; scale  $0''.30$  /px) on the 4m Blanco telescope (CTIO; La Serena). We collected 15  $J$ -band images, each of which was the co-added result of six individual 5 s exposures; these had median seeing  $0''.74$  arcsec. We also obtained 15  $K_s$ -band images, consisting of eight co-added images with individual exposure times of 5 s, and median seeing  $0''.75$  arcsec. The total exposures per band are thus 450 s in  $J$  and 600 s in  $K_s$ .

These data were supplemented with deep NIR data ( $J, K_s$ ) from the Multi-Conjugate Adaptive Optics Demonstrator (MAD) temporarily available on the Very Large Telescope (VLT; ESO, Paranal). MAD is a prototype instrument performing real-time correction for atmospheric turbulence (Marchetti et al. 2006). Its infrared camera employs a  $2048 \times 2048$  Hawaii-II infrared detector with a scale of  $0''.028$  /px for a total FoV of  $\approx 1'$ . During the first Science Demonstration of MAD four  $1' \times 1'$  fields were observed in a region located in the S-W corner of NGC 3201. Five guide stars with visual magnitudes ranging from 11.8 to 12.9 distributed on a circle of 2 arcmin diameter concentric to the field were used. For each pointing we collected three  $J$ -band and five  $K_s$ -band images of 240 sec (DIT=10, NDIT=24). The seeing during the observations changed from 0.6 to 0.9 arcsec ( $J$ -band) and from 0.8 to 1.3 arcsec ( $K_s$ -band). The full width at half-maximum (FWHM) measured on the images ranges from 0.07 to 0.10 arcsec. We ended up with a catalog containing  $\sim 54,100$  stars with at least one measurement in each of two different bands. The top panel of Fig. 1 shows the spatial distribution of the different NIR datasets<sup>17</sup>.

The  $V$  and  $I$  data used in this investigation come from the database of original and archival observations that have been collected, reduced, and calibrated by one of the authors (PBS) in an ongoing effort to provide homo-

geneous photometry on the Landolt (1992) photometric system for a significant fraction of GGCs (Stetson 2000). For NGC 3201, we currently have a catalog consisting of  $\sim 180,000$  stars with at least two measurements in each of  $B$ ,  $V$ , and  $I$ ; these span an area with extreme dimensions on the sky of  $\sim 40'$  (E-W) by  $\approx 50'$  (N-S). These data were obtained in the course of 12 ground-based observing runs with various telescopes, as well as with the Wide Field Planetary Camera 2 (WFPC2) and the Advanced Camera for Surveys Wide Field Camera (ACS-WFC) on the Hubble Space Telescope (HST). The accuracy of the zero-points of the optical catalog is believed to be better than 0.01 mag (see the bottom panel of Fig. 1).

Initial photometry on individual images was performed with DAOPHOT IV, followed by simultaneous photometry for the 359 NIR and the 558 ground-based optical images with ALLFRAME (Stetson, 1994). The HST images were reduced in a separate ALLFRAME run. The instrumental IR magnitudes were transformed into the 2MASS photometric system. The standard error for one observation of one star ranges from  $\sim 0.03$  to  $\sim 0.06$  mag, depending upon the filter ( $J, K$ ) and the night. However, with  $\sim 22,000$  individual observations of more than 1,000 2MASS stars in  $J$  and  $\sim 26,000$  observations in  $K$ , we expect that our results should be on the 2MASS photometric system to  $\lesssim 0.02$  mag in the two bands.

## 3. COMPARISON BETWEEN THEORY AND OBSERVATIONS

The NIR CMDs present the obvious advantage of being minimally affected by uncertain and possibly differential reddening. However, image quality, angular resolution, and photometric precision have partially hampered the use of NIR photometry in crowded fields. Data plotted in the top panel of Fig. 2 show the  $K, J-K$  CMD based on data collected with NIR cameras on 4m telescopes (black dots, SOFI@NTT, ISPI@4m Blanco) and with MAD on VLT (red dots). The error bars plotted in the right side show that the photometric precision is of the order of a few hundredths of a magnitude over most of the magnitude range, increasing to  $\sim 0.1$  mag at our adopted detection limit ( $K \approx 20$ ,  $J \approx 20.7$ ). Note, in particular, that the MS in the low-mass regime shows a well defined knee. This feature is mainly caused by the collisionally induced absorption of  $\text{H}_2$  at NIR wavelengths (Saumon et al. 1994). According to theory, the color and the shape of the bending depends on the metal content. However, the magnitude and color of the bend are, at fixed chemical composition, essentially independent of cluster age. This feature offers the unique opportunity to anchor cluster isochrones, and in turn to estimate the absolute age either as a color or as a magnitude difference between the bend and the cluster TO. The knee is a robust prediction, since for ( $M \approx 0.5\text{--}0.4 M_\odot$ ) the stellar structures are minimally affected by uncertainties in the treatment of convection, given that convective motions are nearly adiabatic (Saumon et al. 2008). In passing we note that a similar feature was already detected in two GCs ( $\omega$  Cen, Pulone et al. 1998; M4, Pulone et al. 1999) and in the Galactic bulge (Zoccali et al. 2000) using deep and high angular resolution NIR ( $J, H$ ) data collected with NICMOS@HST. To estimate the ridge line we represented each star detected in the  $J, K$ -bands by a Gaussian kernel with a sigma equal to the photometric uncertainty. The

<sup>17</sup> Following Harris (1996) we assumed for the center of the cluster the coordinates:  $\alpha = 10^{\text{h}}17^{\text{m}}36^{\text{s}}.8$ ,  $\delta = -46^{\circ}24'40''$

individual Gaussians were summed and we identified the peaks along the MS. This ridge line was smoothed with a spline and the TO (red circle) and the MS knee (MSK, purple circle) were estimated as the points showing the minimum curvature in the two different color ranges (see also Table 1).

To estimate the absolute age of NGC 3201, we have used the new set of isochrones for  $Y = 0.250$ ,  $[\text{Fe}/\text{H}] = -1.50$ , and  $[\alpha/\text{Fe}] \approx 0.4$  from the Vandenberg et al. (2010, in preparation) compilation. [A constant enhancement was not assumed for all  $\alpha$ -elements; rather, the Cayrel et al. (2004) determinations of individual [element/Fe] ratios in metal-deficient stars were adopted.] Fully consistent opacities and the latest nuclear reactions, along with treatments of H/He diffusion and turbulent mixing very close to those described by Proffitt & Vandenberg (1991) and Proffitt & Michaud (1991), respectively, were employed. Moreover, the free parameters in their simple treatment of turbulence were set so that the predicted variation in the surface helium abundance during the main-sequence and subgiant phases agreed well with that reported by Korn et al. (2007). The latter had notable success explaining the observed abundances of a number of the heavy elements, using models that allowed for the settling and radiative accelerations of the metals; consequently, their prediction of the dependence of helium abundance on evolutionary state represents the current best estimate. Although Vandenberg et al. have not treated the diffusion of the metals their isochrones are very similar to those used in the Korn et al. investigation, both morphologically and insofar as the predicted age at a fixed turnoff luminosity are concerned.

The isochrones were transformed from the theoretical to the observed plane using the color-temperature (CT) relations derived by Casagrande, Vandenberg, & Stetson (2010, in preparation) from the latest MARCS model atmospheres (Gustafsson et al. 2008). Small zero-point adjustments (0.03 mag) were applied to colors of the isochrones so that the synthetic colors for stars fainter than the turnoff agreed well with those derived from the IRFM-based, empirical CT relations for dwarf stars by Casagrande et al. (2009). Consistent fits of these isochrones to most of the CMDs for NGC 3201 that can be derived from  $BVRIJK_s$  photometry indicated a clear preference for a true distance modulus  $\mu_0 \sim 13.35 \pm 0.11$  and a reddening  $E(B - V) \approx 0.24 \pm 0.02$ .

The extinction in the NIR bands was estimated using the McCall (2004) relations. The colored lines plotted in the top panel of Fig. 2 show the comparison with three isochrones at  $t = 10, 12$  and 14 Gyr. However, the model isochrones in this CMD appear to be  $\approx 0.05$  mag bluer than observed for magnitudes fainter than the MSK.

To overcome subtle uncertainties in the cluster reddening, we performed a comparison between theory and observations using a Wesenheit  $K$ -band<sup>18</sup> magnitude. This magnitude is reddening free, so the reddening uncertainty in the  $WK, J-K$  CMD occurs only in the horizontal direction. Data plotted in the bottom panel of Fig. 2 show even more clearly the systematic drift in color of cluster isochrones when compared with observations.

<sup>18</sup>  $WK = K - A_K / (A_J - A_K) [J - K]$  mag, where the  $A_J$  and  $A_K$  are the selective absorption according to McCall's relation.

To further constrain the possible culprit(s) for this discrepancy we cross-correlated the NIR ( $J, K$ ) photometry based on MAD images with the optical ( $V, I$ ) photometry based on ACS images. The top panels of Fig. 3 show the  $K, I - K$  (left) and the  $K, V - K$  (right) optical-NIR CMD. Data plotted in these panels display several interesting features. *i*)– The MS knee is still present, although less evident than in the NIR CMD. However, the approach we devised allows us to provide accurate magnitude and color estimates for the age indicators (see Table 1). *ii*)– The same isochrones that in the NIR ( $K, J - K$ ) CMD attain systematically bluer colors fainter than MSK provide—assuming identical values for distance and reddening—a reasonable fit to both evolved and MS stars. However, the isochrones again attain systematically bluer colors below the MS knee ( $K \geq 18.5$  mag). The same outcomes apply if the comparison is performed using the reddening free Wesenheit  $K$ -band magnitude and the same optical-NIR colors (see the bottom panels in Fig. 3).

As a further test of the isochrones we performed the same comparison for an optical  $I, V - I$  CMD. In particular, we took advantage of the deep and precise photometry from ACS and ground-based images. Data in Fig. 4 display a well defined cluster sequence ranging from the subgiant branch to the very low-mass regime ( $I \sim 24$ ,  $V - I \sim 2$  mag). Note that a handful of candidate cluster white dwarfs shows up in the left bottom corner ( $I \sim 24.5$ ,  $V - I \sim 0.25$  mag). The MS knee is less evident than in the optical-NIR CMDs, but both the high number of stars and the photometric precision permit a robust identification of the age indicators (see Table 1). Interestingly, we found that the same isochrones in the NIR and optical-NIR CMDs provide a good fit to the observations over the entire magnitude and color range. The isochrones are only slightly redder for magnitudes fainter than the MSTO. This clearly indicates that optical-NIR, and to a minor extent NIR, CMDs are an acid test of the precision of both evolution and atmosphere models. Even small changes in the input physics can be easily identified in the quoted CMDs.

The comparison between theory and observations highlights two relevant findings: *i*)– the adopted chemical composition is appropriate for NGC3201, since cluster isochrones simultaneously account for both optical and optical-NIR CMDs; *ii*)– the main reason in the discrepancy between theory and observations in the NIR and in the optical-NIR CMDs appears to be the  $K$ -band and to a small extent the  $I$ -band. The isochrones attain colors that are slightly either bluer ( $K, J-K$ ) or redder ( $I, V-I$ ) than the observed MSK. An independent and preliminary test performed using the same isochrones, but a different set of CT relations (Casagrande et al. 2010) show a smaller color discrepancy and very similar cluster ages.

#### 4. RESULTS AND DISCUSSION

The adopted cluster isochrones for ages ranging from 10 to 14 Gyr indicate that the magnitude/age derivative of MSTO stars changes from  $\Delta V / \Delta t \sim 0.093$ , to  $\Delta I / \Delta t \sim 0.080$  and to  $\Delta K / \Delta t \sim 0.062$  mag/Gyr. This means that the age sensitivity decreases by  $\approx 35\%$  when moving from the  $V$  to the  $K$ -band. On the other hand, the color/age derivative of MSTO stars is  $\Delta(V - I) / \Delta t \sim$

0.013 for optical bands,  $\Delta(V - K)/\Delta t \sim 0.032$ ,  $\Delta(I - K)/\Delta t \sim 0.019$  for optical-NIR bands and  $\Delta(J - K)/\Delta t \sim 0.010$  mag/Gyr for NIR bands. These color-age derivatives indicate that optical ( $V - I$ ) and NIR ( $J - K$ ) colors attain similar sensitivities, while the optical-NIR ( $V - K$ ,  $I - K$ ) colors are, as expected, a factor of two-three more sensitive. A decrease of 0.2 dex in iron content implies a  $\sim 20\%$  decrease in magnitude/age derivatives, while an increase of the same amount causes minimal changes ( $\leq 5\%$ ). The same changes in chemical composition have minimal effects on the color/age derivatives.

However, the reddening law by McCall (2004) gives selective absorptions of  $A_I/A_V \sim 0.538$ <sup>19</sup>,  $A_K/A_V \sim 0.112$  mag and reddening corrections of  $E(V - K)/E(V - I) \sim 1.923$ ,  $E(I - K)/E(V - I) \sim 0.923$  and  $E(J - K)/E(V - I) \sim 0.343$  mag. These numbers indicate that the  $K$  magnitudes and  $J - K$  colors are respectively one order of magnitude and more than a factor of two less affected by reddening uncertainties ( $\sim 10\%$ ) than the  $V - I$  colors and the  $I$  magnitudes.

To constrain the error budget in the absolute age estimates of GCs, based on the MSTO, we also need to account for uncertainties affecting the distance determination. The uncertainty in the GC distance depends on the adopted standard candle and is still of the order of 5% (Bono et al. 2008). Using the quoted error budget we estimated the absolute magnitude of the MSTO in the optical and in NIR bands (see Table 1). The error budget on absolute magnitudes is, as expected, dominated by the uncertainties in cluster distances. It is on average  $\sim 0.11$  mag for  $M_K$ ,  $M_I$  and for the Wesenheit magnitudes. The uncertainty of the chemical composition and the cluster isochrones will be discussed in a future paper (Dall’Ora et al. 2010, in preparation). Using the quoted isochrones we found absolute age estimates and uncertainties (see Table 1) for NGC 3201 that agree, within one sigma, with similar estimates in the literature. The weighted mean of the three age estimates based on the  $K$ -band is  $11.48 \pm 1.27$ , while that based on the  $WK$ -band is  $11.55 \pm 1.53$  Gyr. Optical and NIR (see Table 1) age estimates agree within one sigma. The relative ages (De Angeli et al. 2005) are typically affected by smaller

<sup>19</sup> To account for the difference in the effective wavelength between the  $I$ -band adopted by McCall ( $\lambda_{eff}^I = 7977$  Å) and by Landolt ( $\lambda_{eff}^I = 8250$  Å) the selective absorption  $A_I/E(B - V)$  was

errors, but they rely on predictions of evolved evolutionary phases (HB, RGB) affected by different theoretical uncertainties.

We also estimated the absolute ages of NGC 3201 from the difference in magnitude between the MSTO and the MSK using the same approach and the same isochrones. Values listed in Table 1 indicate that ages based on the new method agree, within the errors, with those based on the MSTO. The weighted mean of the three age estimates based on the  $K$ -band is  $10.66 \pm 0.58$  and  $11.63 \pm 0.58$  Gyr based on the  $I$ -band, but the errors are more than a factor of two smaller. The same applies on average to the new age estimates based on the  $WK$  ( $10.82 \pm 0.68$  Gyr) and on the  $WI$ -band. The new age estimates, indeed, do not include uncertainties in the distance and reddening; their uncertainties are dominated by intrinsic photometric errors ( $\sigma_{J,K} \sim 0.02$ ,  $\sigma_{V,I} \sim 0.01 - 0.02$  mag).

The new method to estimate the absolute age of GCs requires accurate NIR photometry  $\approx 2 - 3$  magnitude fainter than the TO region ( $M_J \sim M_K \approx 4 - 6$ ). This means apparent magnitudes  $J \sim K \approx 19 - 21$  mag for a good fraction of GCs and  $J \sim K \approx 14 - 17$  mag for Galactic open clusters. The former limiting magnitudes can be reached with 8-10m class telescopes, while the latter are within the limits of 2-4m class telescopes. However, the Extremely Large Telescopes and JWST will allow us to apply this method to all the stellar systems in the Local Group—provided that suitable, local faint calibrating sequences exist.

We thank C. Brasseur, L. Casagrande and A. Dotter for useful discussions concerning NIR CMDs. This project was supported by Monte dei Paschi di Siena (P.I.: S. Degl’Innocenti), PRIN-INAF2006 (P.I.: M. Bellazzini), PRIN-MIUR2007 (P.I.: G. Piotto). MZ acknowledges Fondap Center for Astrophysics (15010003), CATA PFB-06 and Fondecyt Regular #1085278. We are extremely grateful to ESO for the farsightedness in making available a valuable instrument (MAD) to perform accurate NIR photometry.

changed, following Cardelli et al. (1989), from 1.714 to 1.652.

## REFERENCES

- Asplund M., Grevesse N. & Sauval A.J. 2005, in "Cosmic abundances as records of stellar evolution and nucleosynthesis", ed. F.N. Bash & T.J. Barnes, (San Francisco: ASP), 25
- Bono, G. et al. 2008, ApJ, 2008, 686, L87
- Buoanno, R. et al. 1998, ApJ, 501, 33
- Calamida, A., et al. 2009, in IAU Symp. 'The ages of Stars', 258, 189
- Cardelli, J. A., Clayton, G. C., Mathis, J. S. 1989, 345, 245
- Carraro, G., Girardi, L., Chiosi, C. 1999, MNRAS, 309, 430
- Cayrel, R. et al. 2004, A&A, 416, 1117
- Casagrande, L., Ramirez, I., Melendez, J., Bessell, M., & Asplund, M. 2009, A&A, in press
- Cassisi, S. et al. 1999, A&A, 134, 103
- Castellani, V. 1999, glcl.conf, 109C
- Chaboyer, B. 1998, PhR, 307, 23
- Clement, C. et al. 2001, AJ, 122, 2587
- Covey, K. R. et al. 2003, PASP, 115, 819
- De Angeli, F. et al. 2005, AJ, 130, 116
- Dotter, A. et al. 2008, ApJS, 178, 89
- Gratton, R. et al. 2003, A&A, 408, 529
- Gratton, R., Sneden, C., Carretta, E. 2004, ARA&A, 42, 385
- Grundahl, F., Vandenberg, D. A., Andersen, M. I. 1998, ApJ, 500, 179
- Gustafsson, B., et al. 2008, A&A, 486, 951
- Korn, A., et al. 2007, ApJ, 671, 402
- Kraft, R., Ivans, I. I. 2003, PASP, 115, 143
- Kravtsov, V., Alcano, G.; Marconi, G., Alvarado, F. 2009, A&A, 497, 371
- Layden, A. C., Sarajedini, A. 2003, AJ, 125, 208
- Landolt, A. U. 1992, AJ, 104, 340
- Marchetti, E. et al. 2006, SPIE, 6272, 21
- Mazur, B., Krzemiski, W., Thompson, I. B. 2003, MNRAS, 340, 1205
- McCall, M. L. 2004, AJ, 128, 2144
- Piersimoni, A., Bono, G., Ripepi, V. 2002, AJ, 124, 1528
- Pritzl, B. J., Venn, K. A., Irwin, M. 2005, AJ, 130, 2140
- Proffitt, C. R., & Vandenberg, D. A. 1991, ApJS, 77, 473
- Proffitt, C. R., & Michaud, G. 1991, ApJ, 371, 584

TABLE 1  
MAGNITUDES AND COLORS OF MAIN SEQUENCE TURN-OFF (MSTO) AND MAIN SEQUENCE KNEE (MSK) IN  
DIFFERENT OPTICAL AND NIR CMDs.

CMD	$m_{MSTO}^a$	$CI_{MSTO}^b$	$m_{MSK}^a$	$CI_{MSK}^b$	$M_{MSTO}^c$	$M_{MSK}^c$	$t_{MSTO}^d$	$t_{MSTO-MSK}^e$
<i>K, J-K</i>	16.26	0.41	18.30	0.77	2.83	4.87	$11.8 \pm 2.3$	$10.5 \pm 1.0$
<i>WK, J-K</i>	15.95	0.41	17.77	0.78	2.59	4.41	$12.0 \pm 2.8$	$10.4 \pm 1.1$
<i>K, I-K</i>	16.26	1.06	18.31	1.73	2.83	4.88	$11.8 \pm 2.3$	$10.5 \pm 1.0$
<i>WK, I-K</i>	15.91	1.06	17.72	1.63	2.56	4.37	$11.3 \pm 2.6$	$10.9 \pm 1.2$
<i>K, V-K</i>	16.22	1.96	18.34	3.10	2.78	4.90	$11.0 \pm 2.1$	$11.0 \pm 1.0$
<i>WK, V-K</i>	15.92	1.96	17.81	3.14	2.57	4.46	$11.4 \pm 2.6$	$11.3 \pm 1.2$
<i>I, V-I</i>	17.28	0.91	20.46	1.46	3.53	6.71	$11.5 \pm 2.0$	$11.6 \pm 0.6$
<i>WI, V-I</i>	16.22	0.91	18.71	1.43	2.87	5.36	$11.6 \pm 2.1$	$11.2 \pm 1.2$

<sup>a</sup>Apparent magnitudes of MSTO and MSK.

<sup>b</sup>Color indices of MSTO and MSK.

<sup>c</sup>Absolute magnitudes of MSTO and MSK.

<sup>d</sup>Cluster age estimates (Gyrs) based on the absolute magnitude of MSTO. The uncertainties account for errors on photometry, reddening and distance.

<sup>e</sup>Cluster age estimates (Gyrs) based on the difference in magnitude between MSTO and MSK. The uncertainties account for errors on photometry.

Pulone, L. et al. 1998, ApJ, 492, 41

Pulone, L., De Marchi, G., Paresce, F. 1999, A&A, 342, 440

Renzini, A. 1991, in Observational Tests of Cosmological Inflation, ed. T. Shanks, A.J. Banday & R.S. Ellis (Dordrecht: Kluwer), 131

Richer, H. B. et al. 2006, Sci., 313, 936

Richer, H. et al. 2008, AJ, 135, 2141

Rosenberg, A. et al. 1999, AJ, 118, 230

Rutledge, G. A., Hesser, J. E., Stetson, P. B. 1997, PASP, 109, 907

Salaris, M., Weiss, A. 1998, A&A, 335, 943

Saumon, D. et al. 1994, ApJ, 424, 333

Saumon, D., Marley, M. S. 2008, ApJ, 689, 1327

Stetson, P. B. 1994, PASP, 106, 250

Stetson, P. B. et al. 1999, AJ, 117, 247

Stetson, P. B. 2000, PASP, 112, 925

VandenBerg, D. A., Stetson, P. B., Bolte, M. 1996, ARA&A, 34, 461

VandenBerg, D. A., Clem, J. L. 2003, AJ, 126, 778

VandenBerg, D. A., Bergbusch, P. A., Dowler, P. D. 2006, ApJS, 162, 375

VandenBerg, D. et al. 2008, ApJ, 675, 746

Zoccali, M. et al. 2000, ApJ, 530, 418

Zoccali, M. et al. 2003, A&A, 399, 931

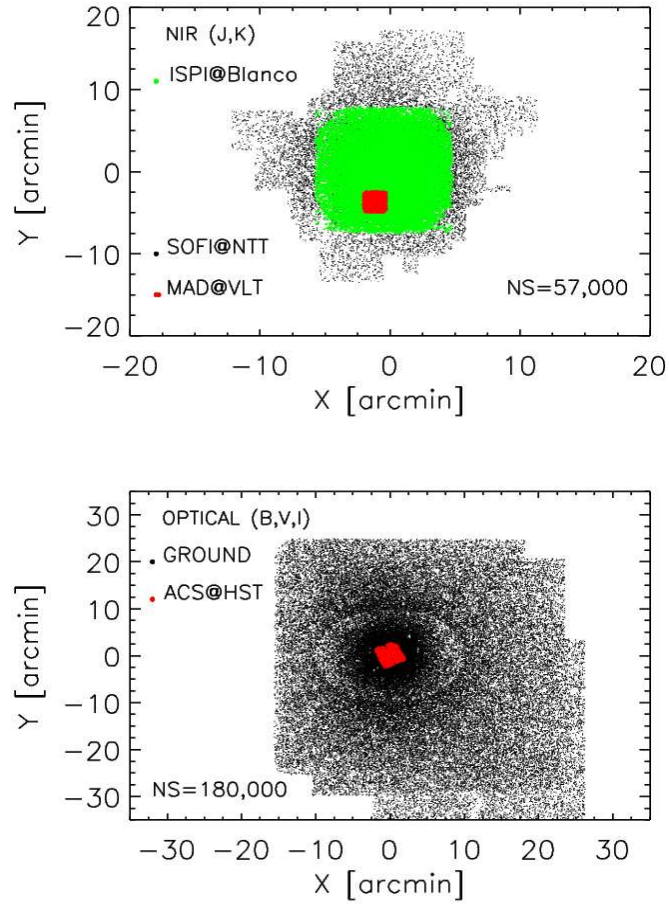


FIG. 1.— Top—Radial distribution of stars observed in the NIR ( $J,K$ ) bands with different ground-based telescopes. Bottom—Same as the top, but for stars observed in the optical ( $V,I$ ) bands with ground-based telescopes and with HST.

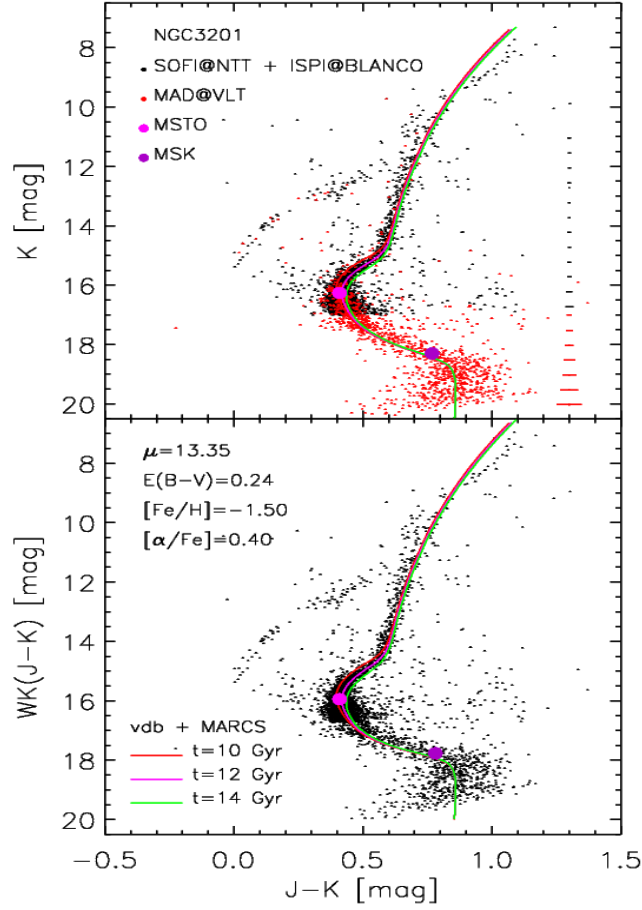


FIG. 2.— Top — NIR ( $K$ ,  $J - K$ ) CMD of NGC3201. Black and red dots display stars observed with SOFI@NTT, ISPI@Blanco and with MAD@VLT. The colored solid lines display a set of cluster isochrones by vandenBerg et al. (2009), at fixed chemical composition, and different ages (see labeled values). These isochrones were transformed into the observational plane using the CT relations based primarily on MARCS model atmospheres (see the text). The adopted true distance and reddening are labeled. The large pink and purple circles mark the position of MS Turn-Off and of the MS knee. Bottom — Same as the top, but using the reddening free  $WK$  magnitude.

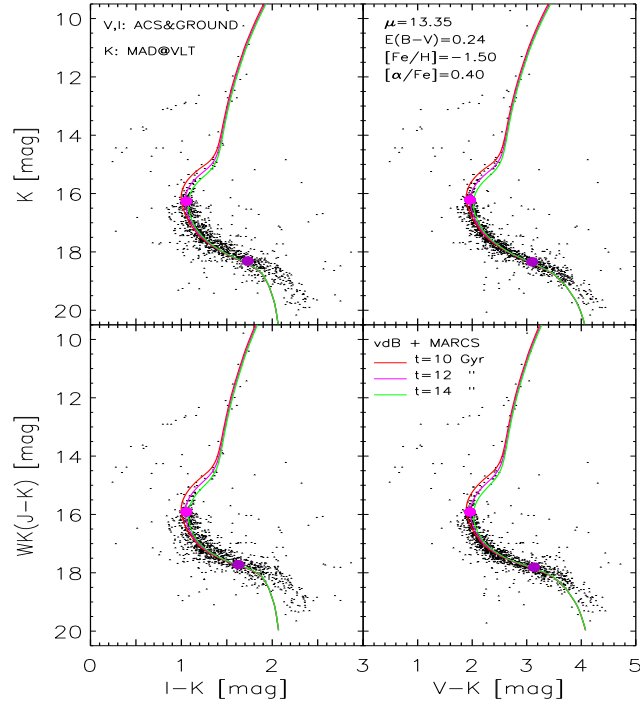


FIG. 3.— Top –  $K$ ,  $I-K$  (left) and  $K$ ,  $V-K$  (right) optical-NIR CMDs of NGC3201. Optical data were collected with ACS-WFC@HST, while the  $K$ -band data were collected with MAD@VLT. Symbols and lines are the same as in Fig. 2. Bottom – Same as the top, but using the reddening free  $W_K$  magnitude.

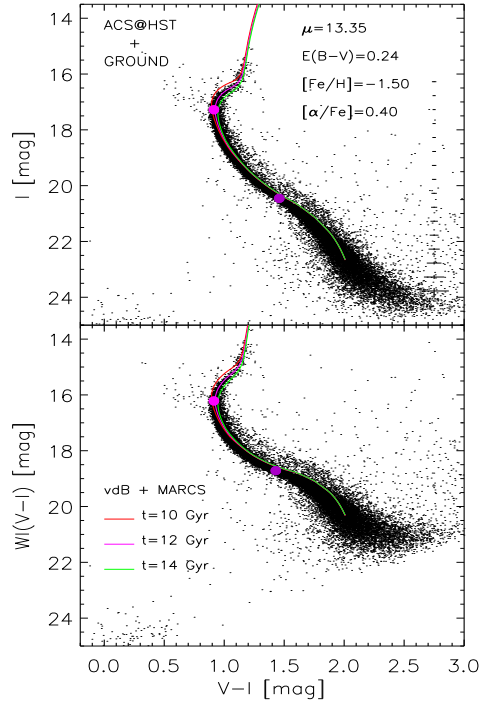


FIG. 4.— Top – Optical  $I$ ,  $V-I$  CMD of NGC3201. Data were collected with ACS-WFC@HST and ground-based telescopes. Symbols and lines are the same as in Fig. 2. The error bars on the right display intrinsic errors in magnitude and color. Bottom – Same as the top, but using the reddening free  $W_I$  magnitude.